Available online at www.sciencedirect.com

ScienceDirect

journal homepage: www.JournalofSurgicalResearch.com

Association for Academic Surgery

Fetal lung transcriptome patterns in an *ex vivo* compression model of diaphragmatic hernia

Zachary D. Fox, BA,[a,1] *Guihua Jiang, MS,*[a,1] *Kenneth K.Y. Ho, BE,*[b] *Kendal A. Walker, BS,*[a] *Allen P. Liu, PhD,*[b] *and Shaun M. Kunisaki, MD, MSc*[a,*]

[a] *Department of Surgery, Michigan Medicine, University of Michigan, Ann Arbor, Michigan*
[b] *Mechanical Engineering, Michigan Medicine, University of Michigan, Ann Arbor, Michigan*

ARTICLE INFO

Article history:
Received 1 March 2018
Received in revised form
26 April 2018
Accepted 20 June 2018
Available online 14 July 2018

Keywords:
Pulmonary hypoplasia
Lung development
Congenital diaphragmatic hernia
Mechanical compression
Periostin

ABSTRACT

Background: The purpose of this study was to employ a novel *ex vivo* lung model of congenital diaphragmatic hernia (CDH) to determine how a mechanical compression affects early pulmonary development.

Methods: Day-15 whole fetal rat lungs (n = 6-12/group) from nitrofen-exposed and normal (vehicle only) dams were explanted and cultured *ex vivo* in compression microdevices (0.2 or 0.4 kPa) for 16 h to mimic physiologic compression forces that occur in CDH *in vivo*. Lungs were evaluated with significance set at $P < 0.05$.

Results: Nitrofen-exposed lungs were hypoplastic and expressed lower levels of surfactant protein C at baseline. Although compression alone did not alter the α-smooth muscle actin (*ACTA2*) expression in normal lungs, nitrofen-exposed lungs had significantly increased *ACTA2* transcripts (0.2 kPa: 2.04 ± 0.15; 0.4 kPa: 2.22 ± 0.11; both $P < 0.001$). Nitrofen-exposed lungs also showed further reductions in surfactant protein C expression at 0.2 and 0.4 kPa (0.53 ± 0.04, $P < 0.01$; 0.69 ± 0.23, $P < 0.001$; respectively). Whereas normal lungs exposed to 0.2 and 0.4 kPa showed significant increases in periostin (*POSTN*), a mechanical stress–response molecule (1.79 ± 0.10 and 2.12 ± 0.39, respectively; both $P < 0.001$), nitrofen-exposed lungs had a significant decrease in *POSTN* expression (0.4 kPa: 0.67 ± 0.15, $P < 0.001$), which was confirmed by immunohistochemistry.

Conclusions: Collectively, these pilot data in a model of CDH lung hypoplasia suggest a primary aberration in response to mechanical stress within the nitrofen lung, characterized by an upregulation of *ACTA2* and a downregulation in *SPFTC* and *POSTN*. This *ex vivo* compression system may serve as a novel research platform to better understand the mechanobiology and complex regulation of matricellular dynamics during CDH fetal lung development.

* *Corresponding author*. Section of Pediatric Surgery, C.S. Mott Children's Hospital, Michigan Medicine, University of Michigan, 1540 E. Hospital Drive, SPC 4211, Ann Arbor, MI 48109. Tel.: +1 734 936 8464; fax: +1 734 936 9784.
E-mail address: shaunkun@umich.edu (S.M. Kunisaki).
[1] These authors contributed equally to this work.
0022-4804/$ – see front matter © 2018 Elsevier Inc. All rights reserved.
https://doi.org/10.1016/j.jss.2018.06.064

Introduction

Pulmonary hypoplasia and pulmonary hypertension continue to be major problems in neonates born with congenital diaphragmatic hernia (CDH). Despite ongoing advances in state-of-the-art care, including fetal tracheal occlusion, extracorporeal membrane oxygenation, and permissive hypercapnia, mortality rates for infants with CDH remain in excess of 30%.[1-4] Among survivors, the pulmonary morbidity associated with this disease can be quite significant, as validated by the spawning of multidisciplinary clinics involving surgeons, pulmonologists, and other specialists at major children's hospitals nationwide.[5] A better understanding of the CDH disease pathogenesis is needed if further inroads are to be made in the management of this debilitating condition.

Until recently, CDH lung hypoplasia has been thought to be primarily caused by mechanical trauma after impaired closure of the pleuroperitoneal canal at 8-wk gestation.[6] The herniated abdominal contents subsequently lead to extrinsic mechanical compression of the lung during the pseudoglandular and canalicular stages of its development. Evidence for this is supported by surgical creation of a diaphragmatic defect in fetal lambs, which has been shown to induce lung hypoplasia.[7] Nevertheless, this classical paradigm has been challenged as being too simplistic based on several important observations.[8] First, despite the fact that the diaphragmatic defect almost always occurs in only one hemidiaphragm, the observed pulmonary hypoplasia and pulmonary hypertension at birth also affect the contralateral lung, albeit to a lesser degree.[9] Second, other space-occupying lesions because of which there is extrinsic mass effect on the early fetal lung (e.g., congenital lung malformations) do not typically result in significant lung hypoplasia and pulmonary hypertension at birth.[10] Finally, teratogenic rodent models of CDH point toward primary aberrations of retinoic acid signaling within the mesenchyme itself as a causative factor in CDH.[11,12]

Given these observations, we sought to better understand the relative contribution of mechanical forces in the CDH lung by exploring lung development in the nitrofen rat model using a novel *ex vivo* mechanical compression microdevice. Our hypothesis was that an *ex vivo* mechanical compression would cause more significant impairment of pulmonary epithelial and mesenchymal development in nitrofen lungs than control lungs.

Methods

Nitrofen CDH rat model

This study was approved by the University of Michigan Unit for Laboratory Animal Medicine under the protocol PRO00007385 in accordance with the National Institute of Health Guidelines for the Care and Use of Laboratory Animals. To induce fetal lung hypoplasia, timed pregnant Sprague-Dawley rats (Charles River, Wilmington, MA) were gavage fed 100 mg of nitrofen (2,4-dichlorophenyl-p-nitrophenyl ether; Sigma-Aldrich, Cat# 33,374, St. Louis, MO), a banned herbicide and known retinoic acid synthesis inhibitor, dissolved in 1 mL of olive oil on gestational day 9 (E9) as previously described in our laboratory.[13] Additional dams were gavage fed 1 mL of olive oil (control vehicle) to provide fetal lung controls (also referred to as "normal lungs"). On day 15 (E15) or day 21 (E21), dams were deeply anesthetized, and all fetuses without regard to sex were harvested by cesarean section. Lungs were dissected out intact in Hank's buffered saline under a dissecting microscope (Fig. 1A).

Rat lung compression device

A microdevice capable of applying compressive stress to fetal rat lung explants was specially designed based on a previously described apparatus (Fig. 1B).[14] Briefly, whole fetal rat lungs were encapsulated in Matrigel (BD, Franklin Lakes, NJ) and placed in a Transwell six-well plate on top of a 0.4-μm pore size PET Transwell filter (07-200-170; Fisher Scientific, Hampton, NH) to allow for nutrient and oxygen diffusion. A sterilized PDMS mold with 24-mm holes was used to make a 1% agarose (UltraPure Agarose, #16500-100; Invitrogen, Carlsbad, CA) cushion overlay. To apply a constant stress (in kPa), a fixed weight was applied over the cushion (Fig. 1C). Although the agarose gel cushion gradually compacts over a 16-h period before stabilizing, this system allows for the total stress of the agarose-explant interface to remain constant throughout the experiments. The explants were randomly divided into six groups (n = 6-12 per group): normal 0 kPa, normal 0.2 kPa, normal 0.4 kPa, nitrofen 0 kPa, nitrofen 0.2 kPa, and nitrofen 0.4 kPa. The pressure settings were selected based on estimates of *in vivo* mechanical forces induced by abdominal herniation into the thorax[15,16] as well as preliminary data demonstrating nonviable lung tissue at 0.6-1.0 kPa.

Lung morphometric analyses

Explants were photographed under an inverted phase-contrast microscope (×4 magnification). Digital images at day 0 (E15), 24 h (E15 + 1), and 48 h (E15 + 2) were blindly analyzed for total lung surface area and terminal lung budding using ImageJ software as previously described.[17] For lung surface area calculations, the outline of the lung explant was manually traced and integrated using the imaging software. For a branching analysis, a terminal bud was defined as a single acinus separated by distinct septa at the periphery of the explant.

Histology

To confirm the CDH phenotype, euthanized fetuses were chosen at random and fixed in 4% paraformaldehyde for 24 h. Coronal sections were performed for hematoxylin and eosin staining. For immunofluorescence analyses, tissue fixation was performed in the same manner for 30 min before paraffin embedding. Five-micron-thick sections underwent antigen retrieval, were incubated with conjugated primary antibodies, and counterstained with 4',6-diamidino-2-phenylindole. Primary antibodies were against E-cadherin (ECAD, 1:500; BD), α-smooth muscle actin (α-SMA/ACTA2, 1:1000; Sigma), Ki67 (1:200; Millipore, Burlington, MA), cleaved caspase-3 (Cas3, 1:200; Cell Signaling Technology, Danvers, MA), and periostin (POSTN, 1:2000; Abcam, Cambridge, UK). Fluorescence

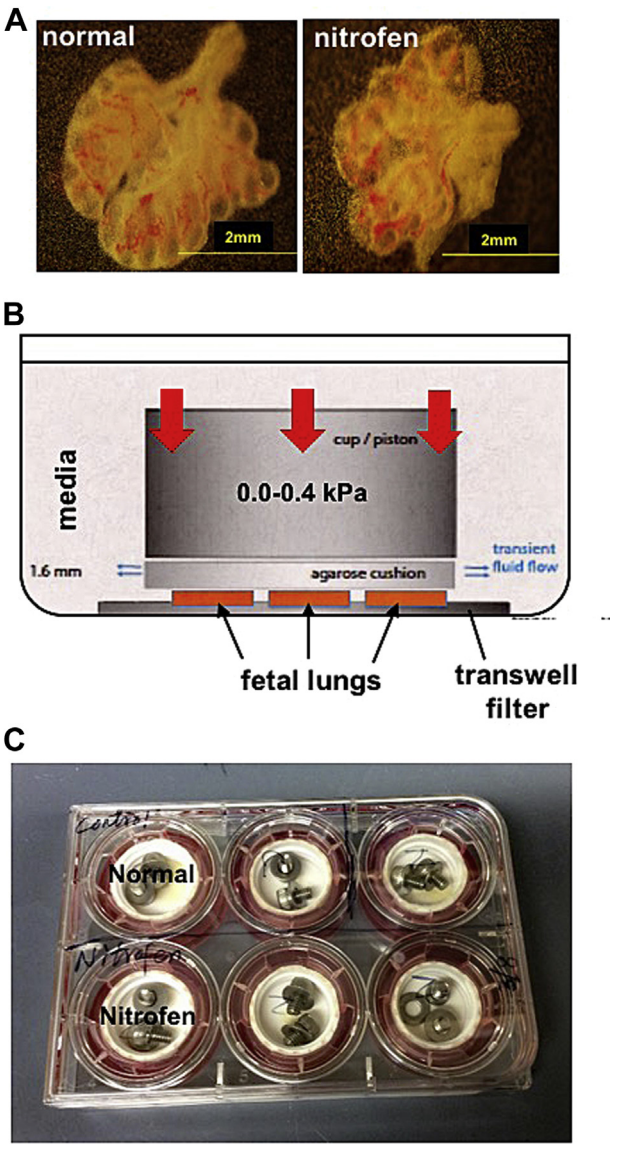

Fig. 1 – *Ex vivo* compression of fetal lungs as a model of congenital diaphragmatic hernia pulmonary development. (A) Representative low-power photomicrographs of harvested fetal lungs at E15 after E9 maternal exposure of control vehicle (*left*) and nitrofen (*right*; magnification, ×4). Scale bar = 2 mm. (B) Schematic diagram of the compression device that allows for controlled delivery of a predetermined static compression force to whole fetal lungs (in orange) at the agarose-tissue interface. Adapted from Tse *et al.*[14] (2012), with no permission required. (C) Photograph of a typical six-well plate compression microdevice used to deliver 0.4 kPa.

microscopy imaging was performed using a Nikon A1 system (Melville, NY).

RNA extraction and quantitative gene expression

Relative gene expression of markers of pulmonary development was analyzed by quantitative reverse transcription polymerase chain reaction. Total RNA was extracted from explants using a MagMAX-96 Total RNA Isolation Kit (Life Technologies, Carlsbad, CA) and MagMAX Express (Applied Biosystems, Foster City, CA). RNA quantity and quality were determined spectrophotometrically, using a NanoDrop 2000 (Thermo Fisher, Waltham, MA). Reverse transcription was conducted using the SuperScript VILO kit (Invitrogen), according to manufacturer's protocol. Finally, a quantitative reverse transcription polymerase chain reaction was performed using the Fast SYBR Green Master Mix (Applied Biosystems) and AB-QuantStudio 3 real-time PCR machine (Thermo Fisher). *ACTB* was used as a reference gene for the normalization of target gene expression using the $2^{-\Delta\Delta Ct}$ method. Rat-specific PCR primers were designed using Primer-BLAST (http://www.ncbi.nlm.nih.gov/tools/primer-blast/). The following are the designed primer sequences: surfactant protein B (SFPTB) forward: 5′CCA GTG AAC AGG CTA TGC CA3′, SFPTB reverse: 5′CTG CTC ACA CTT TTG CCT GTC3′; surfactant protein C (SFPTC) forward: 5′CCC ACC GGA TTA CTC GAC AG3′, SFPTC reverse: 5′CCA CCA CAA CCA CGA TGA GA3′; ACTA2 forward: 5′GGC CAC TGC TGC TTC CTC TTC TT3′, ACTA2 reverse: 5′TGC CCG CCG ACT CCA TTC3′; POSTN (21/22) forward: 5′TGC AAA AAG ACA CAC CTG CAA3′, POSTN (21/22) reverse: 5′GGC CTT CTC TTG ATC GCC TT3′; TGF-β1 forward: 5′CTG CTG ACC CCC ACT GAT AC3′, TGF-β1 reverse: 5′ AGC CCT GAT TTC CGT CTC CT3′; ACTB forward: 5′TTG CTG ACA GGA TGC AGA AG3′, ACTB reverse: 5′TAG AGC CAC CAA TCC ACA CA3′.

Statistical analyses

Quantitative data were presented as the mean ± SEM. Data were analyzed by the Student's *t*-test or one-way analysis of variance with post hoc testing by Dunnett correction for multiple comparisons, as appropriate, using Prism 6 (GraphPad, La Jolla, CA). Results were considered to be statistically significant if $P < 0.05$.

Results

Nitrofen-exposed fetal lungs are hypoplastic and express POSTN

Maternal nitrofen exposure reliably induced the CDH phenotype in fetuses at term, as evidenced by herniation of abdominal viscera into the thoracic cavity (Fig. 2A). Nitrofen exposure was also associated with fetal lung hypoplasia as demonstrated by a decreased percent of lung weight relative to body weight compared to age-matched fetuses exposed to control vehicle (2.0 ± 0.06% *versus* 3.9 ± 0.24%, respectively; $P < 0.0001$; Fig. 2B).

To assess the maturity of pulmonary distal epithelial cells in fetal lungs, we evaluated *SFPTC* expression. Nitrofen exposure was associated with a significant reduction in *SFPTC* when compared to control vehicle lungs at term (3874 ± 110 *versus* 6699 ± 529, respectively; compared to housekeeping gene; $P = 0.0004$). Conversely, the expression of *ACTA2*, the gene encoding for α-SMA, was significantly increased in nitrofen-exposed lungs compared to control vehicle (30.1 ± 1.7

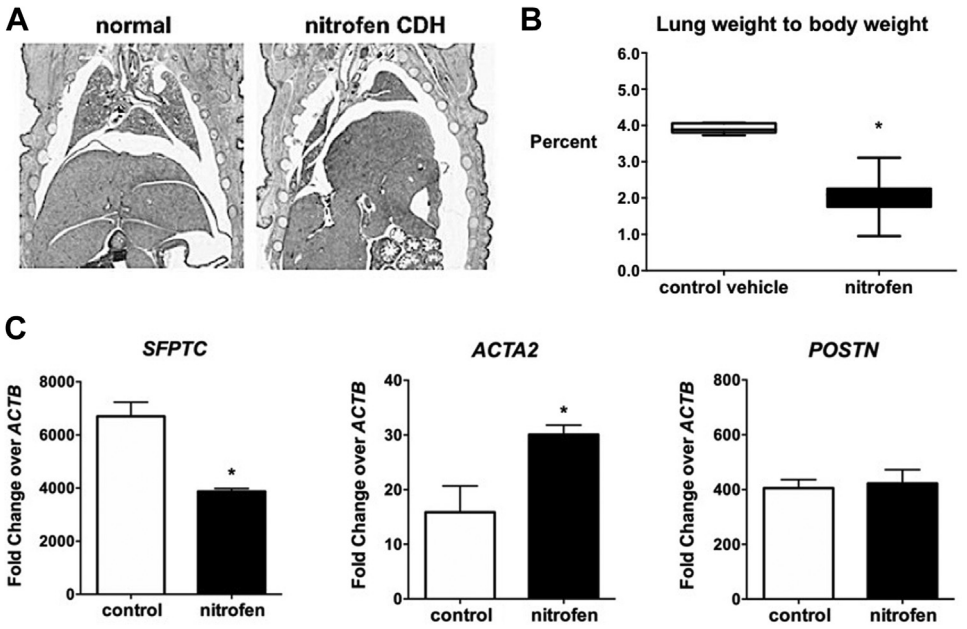

Fig. 2 – Baseline characteristics of term lungs in the nitrofen model of fetal congenital diaphragmatic hernia lung hypoplasia. (A) Hematoxylin and eosin staining of coronal sections through the fetal rat torso at E21 revealed normal anatomy (*left*) after exposure to control vehicle in contrast to liver herniation with lung hypoplasia (*right*) after exposure to nitrofen (magnification, ×4). (B) Lung weight relative to body weight (expressed as a percent) in control vehicle versus nitrofen-exposed E21 fetal rats ($n = 7$/group). Data are presented as mean ± SEM, and the asterisk denotes statistical significance (t-test, $P < 0.05$) compared to control vehicle fetal lung values. (C) Relative levels of surfactant protein C (*SFPTC*), α-smooth muscle actin (*ACTA2*), and periostin (*POSTN*) mRNA expression among E21 fetal lungs ($n = 5$/group) revealed significant differences in epithelial and smooth muscle development after nitrofen exposure but no differences in baseline *POSTN*. Data are normalized relative to the housekeeping gene, *ACTB*. The asterisk (*) denotes statistical significance (t-test, $P < 0.05$) compared to control fetal lung values, $n = 3$ independent biological replicates.

versus 15.9 ± 4.8, respectively; compared to housekeeping gene; $P = 0.0196$, Fig. 2C) at term. There was no significant difference in *POSTN* expression in term nitrofen-exposed fetal lungs compared with that in control vehicle lungs ($P = 0.776$; Fig. 2C). Taken together, these data suggest that term nitrofen-exposed fetal lungs with CDH are hypoplastic based on size, morphology, and epithelial maturity. Moreover, term nitrofen-exposed lungs have increased myofibroblast gene expression but comparable *POSTN* levels when compared with normal fetal lungs.

Ex vivo *compression inhibits airway branching in the early nitrofen-exposed fetal lung*

To examine the effect of mechanical compression forces on early fetal lung development, we explanted fetal lungs at E15. Using ECAD to stain the pulmonary epithelium, there was evidence for relatively low POSTN expression within the interstitium of both E15 control vehicle and nitrofen-exposed lung tissue in the absence of compression (Fig. 3A). Quantitative assessment of lung *POSTN* gene expression confirmed these findings in control vehicle and nitrofen-exposed pups (66.2 ± 3.0 and 62.7 ± 3.8, respectively, compared to housekeeping gene; $P = 0.49$). Figure 3B shows that *SFPTB* and *SFPTC* transcripts in control vehicle lungs were significantly increased compared with those in nitrofen-exposed lungs at E15 (*SFPTB*: 5.0 ± 0.41 *versus* 1.8 ± 0.08, respectively; *SFPTC*: 151.6 ± 14.0 *versus* 63.8 ± 2.1, respectively; compared to housekeeping gene; both $P < 0.01$). There was no significant difference in *ACTA2* expression at E15 ($P = 0.42$).

Lung morphometric data are shown in Figures 4 and 5. At baseline, E15 nitrofen-exposed lungs showed a significant reduction in total lung surface area when compared with control vehicle lungs (1.67 ± 0.08 *versus* 2.25 ± 0.11 million pixels, respectively; $P < 0.0002$; Fig. 4A). There was a similar reduction in terminal bud number (10.4 ± 1.1 *versus* 13.6 ± 1.4 buds, respectively; $P < 0.05$; Fig. 5A). Fetal lungs that were maintained *ex vivo* under standard culture conditions for 24 h led to increased lung surface area and terminal bud number in nitrofen-exposed and control vehicle lungs (lung surface area: 2.2 ± 0.39 *versus* 3.3 ± 0.33 million pixels, respectively; terminal bud: 13.4 ± 1.1 *versus* 15.0 ± 2.0 buds, respectively), but the relative differences between the two groups remained.

Fetal lung explants were then subjected to *ex vivo* testing in compression microdevices to mimic *in utero* compression from the adjacent abdominal viscera. As expected, control vehicle and nitrofen-exposed lungs had increased lung surface area at 0.2 kPa compared with that at 0 kPa (Fig. 4B). Although some interval lung growth may have occurred, the observed increase in lung surface area was likely secondary to 3D mechanical deformation of the tissue under pressure. No statistical differences were noted between normal and nitrofen-exposed lungs at 0 kPa ($P = 0.28$). Although the impact of mechanical compression on terminal branching

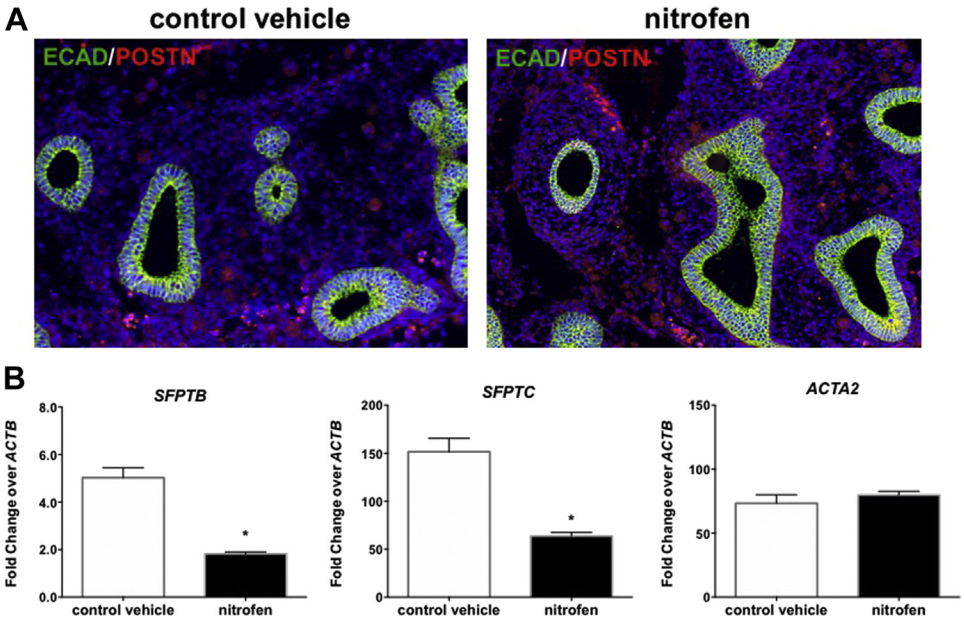

Fig. 3 – Baseline characteristics of E15 (pseudoglandular stage) fetal lungs in the nitrofen model of fetal congenital diaphragmatic hernia lung hypoplasia. (A) Representative fluorescence microscopy images of explanted E15 fetal lungs maintained in culture without compression. Lungs exposed to control vehicle (*left*) and nitrofen (*right*) showed comparable immunostaining patterns of E-cadherin (ECAD, green) within the airways and periostin (POSTN, red) in the lung interstitium. Nuclei were counterstained with 6-diamidino-2-phenylindole (magnification, ×40). (B) Relative levels of surfactant protein B (*SFPTB*), surfactant protein C (*SFPTC*), and α-smooth muscle actin (*ACTA2*) mRNA expression within E15 fetal lungs ($n = 6$/group) revealed significant differences in epithelial and smooth muscle development after nitrofen exposure. Data are normalized relative to housekeeping gene (*ACTB*). The asterisk (*) denotes statistical significance (t-test, $P < 0.05$) compared to control fetal lung values, $n = 3$ independent biological replicates.

was variable in normal lungs, compression resulted in a consistent and significant reduction in terminal budding in nitrofen-exposed lungs (0.4 kPa: 13.0 ± 1.06 and 18.83 ± 1.07 buds in nitrofen and normal lungs, respectively; $P = 0.0028$; Fig. 5B).

Compression uniquely alters the pulmonary transcriptome pattern within the early nitrofen-exposed fetal lung

To determine the effects of mechanical compression on fetal pulmonary transcriptome patterns, pulmonary epithelial and mesenchymal gene expression were assessed on E15 lung explants using different compression forces. Although *SFPTB* levels remained relatively unchanged (Fig. 6A), there was a significant reduction in *SFPTC* expression in nitrofen-exposed lungs (0.2 kPa: 0.53 ± 0.04; 0.4 kPa: 0.69 ± 0.23; both $P < 0.01$; Fig. 6B). Differences in *SFPTC* gene expression were not observed in control vehicle lungs under the same pressure settings. We then assessed for alterations in α-SMA expression under mechanical compression and found that nitrofen-exposed lungs were uniquely associated with significantly increased *ACTA2* at both 0.2 and 0.4 kPa (2.04 ± 0.15 and 2.22 ± 0.10, respectively; both $P < 0.001$ compared to 0 kPa; Fig. 6C). In contrast, control vehicle lungs exposed to increased compression showed no significant change in *ACTA2* expression compared with control lungs at 0 pKa.

Compression modulates POSTN *and* TGF-β *expression within the early nitrofen-exposed fetal lung*

Fluorescence microscopy images of E15 fetal lung tissue exposed to 0.2-0.4 kPa of mechanical compression showed robust evidence of proliferating airway epithelium, as denoted by expression of Ki67, as well as apoptosis of mesenchymal cells based on expression of Cas3 (Fig. 7). To further evaluate the effect of compression within the lung interstitium, expression of POSTN was evaluated in nitrofen-exposed and control vehicle controls within compression microdevices. Nitrofen-exposed lungs showed a relative paucity of POSTN adjacent to areas of α-SMA under the same compression conditions. In contrast, POSTN was uniformly expressed within the mesenchyme in compressed normal lungs (Fig. 7).

Quantitative gene expression supported the immunohistochemistry data, revealing significant increases in *POSTN* expression (1.79 ± 0.10 and 2.12 ± 0.39, both $P < 0.001$) in E15 control vehicle lungs exposed to 0.2 and 0.4 kPa, respectively. In contrast, compressed E15 nitrofen-exposed lungs had a more variable response demonstrating significant decreases in *POSTN* expression (0.4 kPa: 0.67 ± 0.15, $P < 0.001$) than nitrofen-exposed lungs at 0 kPa (Fig. 8A) in two of three experiments performed. *TGF-β1*, a known inhibitor of lung bud development and gene closely related to *POSTN*, was significantly increased in E15 nitrofen-exposed lungs at both 0.2 and 0.4 kPa (1.17 ± 0.12 and 1.36 ± 0.07, respectively; $P = 0.045$;

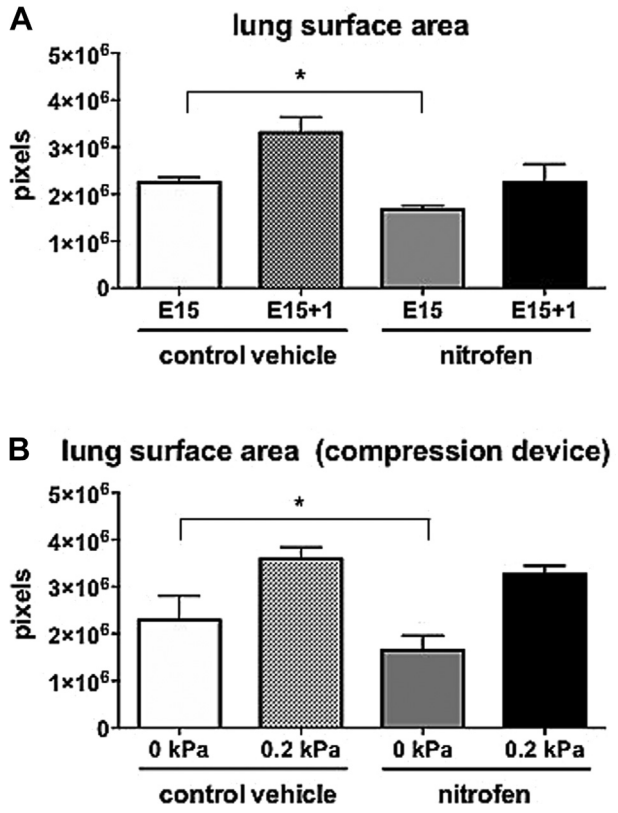

Fig. 4 – Comparative analysis of total lung surface area (measured in pixels) in normal (control vehicle) and nitrofen-exposed fetal lungs cultured *ex vivo* at E15 (n = 3-12/group). (A) Lung surface area was significantly decreased in nitrofen-exposed lungs compared with that in normal lungs at baseline (E15). Lung surface area increased in both the groups after 24 h in culture (E15 + 1) in the absence of compression. Data are presented as mean ± SEM, and the asterisk (*) denotes statistical significance (t-test, $P < 0.05$) compared to E15 normal lungs ($n = 3$ independent biological replicates). (B) Normal and nitrofen-exposed lungs in compression devices demonstrated increased lung surface area at 0.2 kPa compared with that at 0 kPa confirming mechanical flattening of the 3D tissue. The asterisk (*) denotes statistical significance (t-test, $P < 0.05$) compared to E15 normal lungs at 0 kPa ($n = 2$ independent biological replicates).

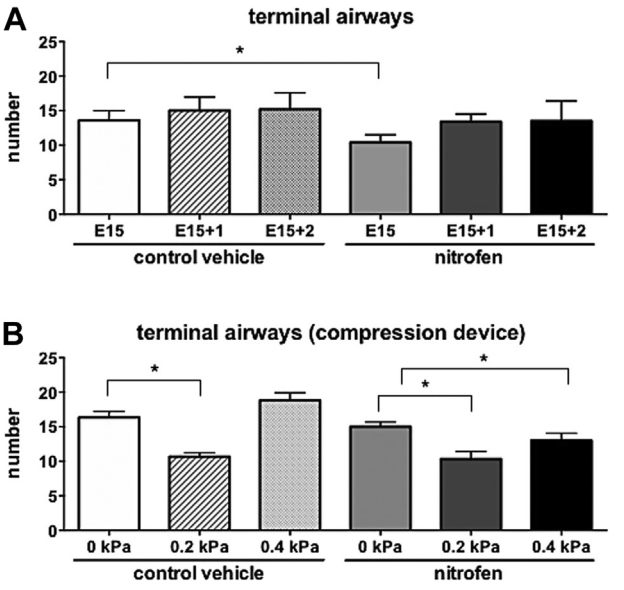

Fig. 5 – Comparative analysis of terminal branching in normal (control vehicle) and nitrofen-exposed fetal lungs cultured *ex vivo* at E15 (n = 3-12/group). (A) The number of terminal buds was significantly decreased in nitrofen-exposed lungs compared with that in normal lungs at baseline (E15). Lung surface area was increased in both the groups after 24 and 48 h in culture (E15 + 1 and E15 + 2, respectively) in the absence of compression. Data are presented as mean ± SEM, and the asterisk (*) denotes statistical significance (t-test, $P < 0.05$) compared to E15 normal lungs ($n = 3$ independent biological replicates). (B) Lungs in compression devices demonstrated impaired terminal airway formation in nitrofen-exposed lung tissue at both 0.2 and 0.4 kPa. The asterisks (*) denote statistical significance (Dunnett, $P < 0.05$) compared to corresponding lungs at 0 kPa ($n = 2$ independent biological replicates).

Fig. 8B). Similarly, E15 control vehicle showed a significant increase in *TGF-β1* transcripts at 0.4 kPa (1.26 ± 0.13, $P = 0.036$).

Discussion

Although significant advances have been made in the management of CDH over the past several decades, the morbidity and mortality in affected neonates remain high because of pulmonary hypoplasia and pulmonary hypertension.[18] Historically, the abnormal development of the CDH lung has been thought to be primarily caused by mechanical compression upon failed closure of the pleuroperitoneal canal at 8-wk gestation,[6] and *in utero* surgical closure of the diaphragm can accordingly dramatically improve the condition in some patients.[19] However, other investigators have long argued that the abnormal CDH lung is likely a part of a more global embryopathy, in which a more basic disturbance affects multiple organs, and that there is a common pathogenetic link among the malformations clustered in CDH patients.[20] A "dual hit" hypothesis has therefore been proposed, whereby fetal lung hypoplasia results from the physical impedance of herniated abnormal tissue exacerbating already inherent abnormalities within the lung mesenchyme in association with CDH-associated genes.[21]

In this pilot study, we used a novel, *ex vivo* lung compression microdevice to specifically study the effect of mechanical forces on pulmonary gene expression within E15 fetal rat lungs. Our major finding was that static mechanical pressure impaired lung development, both in terms of pulmonary transcriptome patterns and terminal branching. Furthermore, disturbances in epithelial cell development, as measured by

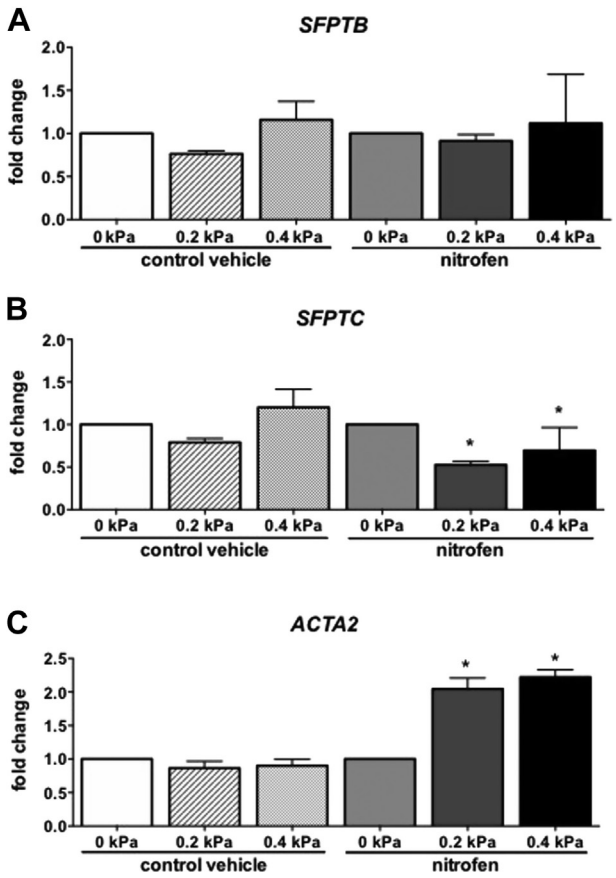

Fig. 6 – Quantitative gene expression after exposure of E15 fetal lungs to mechanical compression (0.2 or 0.4 kPa) based on (A) surfactant protein B (*SFPTB*), (B) surfactant protein C (*SFPTC*), and (C) α-smooth muscle actin (*ACTA2*) mRNA transcripts ($n = 5$/group). Nitrofen-exposed lungs showed significant decreases in *SPFTC* and significant increases in *ACTA2* levels under increased compression. The changes in gene expression were not seen after mechanical compression of control vehicle lung tissue. Levels are normalized values expressed in terms of fold change compared to respective lungs at 0 pKa. The asterisks (*) denote statistical significance (Dunnett, $P < 0.05$) compared to respective lungs at 0 pKa, $n = 3$ independent biological replicates.

SFPTC gene expression, were most significant in nitrofen-exposed lungs under identical conditions. Based on our E21 results and data from others,[22] surfactant deficiency is known to be persistent both in late-term nitrofen-exposed fetal rats and in some neonates with CDH.[23]

We harvested and cultured fetal lungs in our microdevices at E15, believing that this time point would best simulate when lungs would be initially exposed to higher than normal compression forces *in vivo*. The choice of this time point is further supported by genetic mouse models of fetal CDH, which have suggested that the first signs of overt abdominal herniation into the thoracic cavity appear at E16.[24] Interestingly however, our study corroborates with works by others demonstrating that nitrofen-exposed lungs are already hypoplastic and surfactant deficient at the time of fetal diaphragm closure.[22] Evidence for abnormal pulmonary branching morphogenesis occurring as early as E11 has been shown.[22,25,26] These data provide further evidence that a genetic disruption, possibly related to retinoic acid signaling, impairs diaphragmatic closure while simultaneously affecting early pulmonary development. The exact molecular mechanisms in this process have remained elusive.[12,24,27]

Another intriguing finding from our study was the observation that *ACTA2*, the gene associated with α-SMA, was markedly upregulated in nitrofen-exposed lungs within our microdevices. In contrast, *ACTA2* remained relatively unchanged in normal lungs under identical compression conditions. These data are consistent with increased *ACTA2* expression observed in late-term, nitrofen-exposed fetal rats and increased muscularization of the pulmonary vasculature, another key component of the CDH lung phenotype.[28] Although an underlying dysfunction of resident lung mesenchymal progenitors in CDH has been suggested by a number of investigators,[8,21,24,29] our approach to manipulate smooth muscle gene expression using mechanical devices is novel and strengthens the concept that aberrant mesenchymal responses to compression stimuli are playing a synergistic role in further impairing development of the CDH lung. Based on our immunofluorescence data on Cas3 expression, we speculate that compression forces may be inducing lung mesenchymal apoptosis in similar fashion to that observed with nitrofen,[8,21,24,30] thereby disrupting critical epithelial-mesenchymal progenitor interactions required for local epithelial cell activation and normal branching morphogenesis of the airways. The downstream effect of this compression on genes associated with blood vessel maturation, and pulmonary hypertension (e.g., SMAD9) remains an exciting avenue for further exploration.

As expected, our data also found that *TGF-β1* and *POSTN*, also known as osteoblast-specific factor 2, are upregulated in normal lung tissue exposed to mechanical compression. Similar findings of increased *POSTN* gene expression induced by mechanical stimulation have been shown in other disease models and have been implicated in the pathophysiology of abdominal aortic aneurysms and myocardial infarction, among others.[31,32] The aberrant changes in *POSTN* within nitrofen-exposed fetal lung tissue in this microenvironment are especially intriguing because POSTN is a mechanical stress–response protein. Recently, investigators have shown that POSTN is widely expressed by mesenchymal cells during the saccular stage of lung development and is coincident with the accumulation of α-SMA myofibroblasts.[33] Studies have shown that *POSTN* may play an important role in normal alveolar septation and can function as a ligand for $\alpha_v\beta_3$ and $\alpha_v\beta_5$ integrins, thereby having pleiotropic effects in supporting adhesion and migration of epithelial cells.[34,35] Others have demonstrated that *POSTN* potentiates the effects of the TGF-β family of peptides, which are known to exert inhibitory effects on lung epithelial cell proliferation and to cause epithelial-to-mesenchymal transition during terminal bud morphogenesis.[36]

Taken together, this report departs from current paradigms used to study CDH by demonstrating the use of a unique research tool in understanding the mechanobiology of

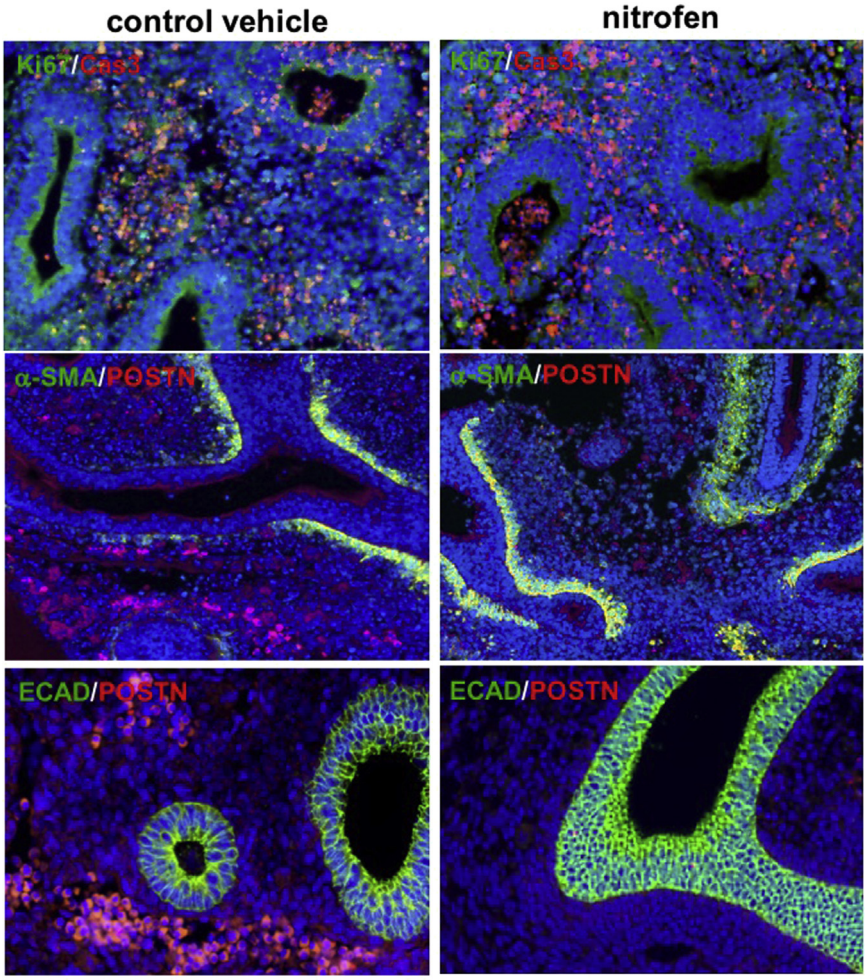

Fig. 7 – Representative fluorescence microscopy images of E15 fetal lungs under mechanical compression forces (0.2-0.4 kPa). Nuclei were counterstained with 6-diamidino-2-phenylindole. Lungs exposed to control vehicle (*top left*) or nitrofen (*top right*) displayed robust evidence of proliferating airway epithelium denoted by expression of Ki67 (green) as well as apoptosis within the interstitium based on expression of cleaved caspase-3 (Cas3, red; magnification, ×20). Nitrofen-exposed lungs (*middle right*) showed a relative paucity of periostin (POSTN, red) adjacent to areas of α-smooth muscle actin (α-SMA, green) immunostaining when compared to compressed control vehicle lungs (*middle left*) under the same compression forces (magnification, ×20). Higher power fluorescence microscopy images revealed E-cadherin (ECAD, green) immunostaining of the airways and robust POSTN (red) expression in compressed control vehicle lungs (*bottom left*) when compared to expression in compressed nitrofen-exposed lungs (*bottom right*, magnification, ×40).

the CDH lung, and future work may ultimately help scientists gain better mechanistic insight required to design new therapeutic targets. Nevertheless, we do acknowledge several caveats and limitations of this study that warrant mention. First and foremost, as with most animal models produced using teratogenic compounds, there may be some heterogeneity in the disease phenotype of nitrofen-exposed CDH lungs, including an absence of any hernia defect in a small fraction of hypoplastic lungs. Moreover, because nitrofen has not been directly implicated in human lung hypoplasia, our rat model may not reliably recapitulate the disease pathogenesis of the CDH lung seen clinically.[37,38] For this reason, studies are ongoing in the laboratory investigating the use of human CDH lung tissue as well as stem cell–derived organoid technologies. In the latter approach, reprogrammed stem cells from afflicted children may allow for a more accurate representation of the patient-specific effects of pressure on fetal lung development. Whether compression forces affect the ipsilateral lung to the same degree as forces on the contralateral lung also merits investigation. In addition, given the impact of "fetal breathing" that commences during the canalicular stage of lung development,[39] whether dynamic mechanical compression better mimics the fetal CDH environment *in vivo* remains unclear. Finally, because we studied hypoplastic fetal lungs at a specific gestational age under a relatively short duration of mechanical stress, we are currently exploring how variations in lung gestational ages and mechanical pressures affect CDH lung growth within these microdevices.

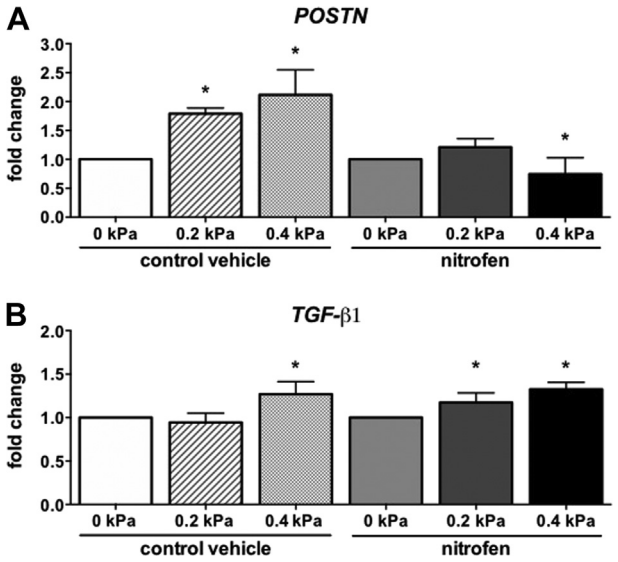

Fig. 8 – Quantitative gene expression after exposure of E15 fetal lungs to mechanical compression (0.2 or 0.4 kPa) based on (A) periostin (*POSTN*) and (B) transforming growth factor-β1 (*TGF-β1*) mRNA transcripts (n = 3-12/group). Compressed normal lungs showed increased levels of *POSTN* and *TGF-β1* expression, whereas compressed nitrofen-exposed lungs typically had significantly diminished *POSTN* transcripts. Levels are normalized values expressed in terms of fold change compared to respective tissue at 0 pKa. The asterisks (*) denote statistical significance (Dunnett, $P < 0.05$) compared to respective tissue at 0 pKa, $n = 3$ independent biological replicates.

Conclusions

Data from this novel *ex vivo* model of CDH fetal lung development suggest a primary aberration in the pulmonary transcriptome pattern within nitrofen-exposed lungs in response to mechanical stress. These findings are associated with impaired upregulation of *POSTN*, a mechanical stress–response protein important for normal lung development. Further investigation of this bioengineering research platform is warranted to help facilitate a better understanding of the effect of mechanical compression on fetal lung growth and matricellular dynamics.

Acknowledgment

The authors would like to thank Julie Di Bernardo, PhD, and Michael Maiden for their technical assistance with the nitrofen rat model. Funding for this project was made possible by the Department of Surgery, Michigan Medicine.

Authors' contributions: Z.D.F., G.J., A.P.L., and S.M.K. contributed to the study conception and design. Z.D.F., G.J., K.K.Y.H., and K.A.W. acquired the data. Z.D.F., G.J., and S.M.K. performed the analysis and interpreted the data. Z.D.F., G.J., and S.M.K. drafted the manuscript. S.M.K. critically revised the article.

Disclosure

There are no disclosures or competing interests for any of the authors of this manuscript.

REFERENCES

1. Wung JT, Sahni R, Moffitt ST, Lipsitz E, Stolar CJ. Congenital diaphragmatic hernia: survival treated with very delayed surgery, spontaneous respiration, and no chest tube. *J Pediatr Surg*. 1995;30:406–409.
2. Does extracorporeal membrane oxygenation improve survival in neonates with congenital diaphragmatic hernia? The congenital diaphragmatic hernia study group. *J Pediatr Surg*. 1999;34:720–724. discussion 724-5.
3. Lally KP, Lally PA, Lasky RE, et al. Defect size determines survival in infants with congenital diaphragmatic hernia. *Pediatrics*. 2007;120:e651–e657.
4. Harrison MR, Keller RL, Hawgood SB, et al. A randomized trial of fetal endoscopic tracheal occlusion for severe fetal congenital diaphragmatic hernia. *N Engl J Med*. 2003;349:1916–1924.
5. Muratore CS, Kharasch V, Lund DP, et al. Pulmonary morbidity in 100 survivors of congenital diaphragmatic hernia monitored in a multidisciplinary clinic. *J Pediatr Surg*. 2001;36:133–140.
6. Wells LJ. A study of closure of the pleuropericardial and pleuroperitoneal canals in the human embryo. *Anat Rec*. 1947;97:428.
7. Harrison MR, Bressack MA, Churg AM, de Lorimier AA. Correction of congenital diaphragmatic hernia in utero. II. Simulated correction permits fetal lung growth with survival at birth. *Surgery*. 1980;88:260–268.
8. Jesudason EC. Small lungs and suspect smooth muscle: congenital diaphragmatic hernia and the smooth muscle hypothesis. *J Pediatr Surg*. 2006;41:431–435.
9. Rottier R, Tibboel D. Fetal lung and diaphragm development in congenital diaphragmatic hernia. *Semin Perinatol*. 2005;29:86–93.
10. Derderian SC, Jayme CM, Cheng LS, Keller RL, Moon-Grady AJ, MacKenzie TC. Mass effect alone may not explain pulmonary vascular pathology in severe congenital diaphragmatic hernia. *Fetal Diagn Ther*. 2016;39:117–124.
11. Raub JA, Mercer RR, Kavlock RJ, Setzer CJ. Effects of prenatal nitrofen exposure on postnatal lung function in the rat. *Prog Clin Biol Res*. 1983;140:119–134.
12. Jay PY, Bielinska M, Erlich JM, et al. Impaired mesenchymal cell function in Gata4 mutant mice leads to diaphragmatic hernias and primary lung defects. *Dev Biol*. 2007;301:602–614.
13. Di Bernardo J, Maiden MM, Hershenson MB, Kunisaki SM. Amniotic fluid derived mesenchymal stromal cells augment fetal lung growth in a nitrofen explant model. *J Pediatr Surg*. 2014;49:859–864. discussion 864-5.
14. Tse JM, Cheng G, Tyrrell JA, et al. Mechanical compression drives cancer cells toward invasive phenotype. *Proc Natl Acad Sci U S A*. 2012;109:911–916.
15. Harding R, Hooper SB. Regulation of lung expansion and lung growth before birth. *J Appl Physiol*. 1985;1996:209–224.
16. Yang EY, Allmendinger N, Johnson SM, Chen C, Wilson JM, Fishman SJ. Neonatal thoracoscopic repair of congenital

diaphragmatic hernia: selection criteria for successful outcome. *J Pediatr Surg*. 2005;40:1369–1375.
17. Di Bernardo J, Maiden MM, Jiang G, Hershenson MB, Kunisaki SM. Paracrine regulation of fetal lung morphogenesis using human placenta-derived mesenchymal stromal cells. *J Surg Res*. 2014;190:255–263.
18. Puligandla PS, Grabowski J, Austin M, et al. Management of congenital diaphragmatic hernia: a systematic review from the APSA outcomes and evidence based practice committee. *J Pediatr Surg*. 2015;50:1958–1970.
19. Harrison MR, Adzick NS, Longaker MT, et al. Successful repair in utero of a fetal diaphragmatic hernia after removal of herniated viscera from the left thorax. *N Engl J Med*. 1990;322:1582–1584.
20. Molenaar JC, Bos AP, Hazebroek FW, Tibboel D. Congenital diaphragmatic hernia, what defect? *J Pediatr Surg*. 1991;26:248–254.
21. Keijzer R, Liu J, Deimling J, Tibboel D, Post M. Dual-hit hypothesis explains pulmonary hypoplasia in the nitrofen model of congenital diaphragmatic hernia. *Am J Pathol*. 2000;156:1299–1306.
22. Guilbert TW, Gebb SA, Shannon JM. Lung hypoplasia in the nitrofen model of congenital diaphragmatic hernia occurs early in development. *Am J Physiol Lung Cell Mol Physiol*. 2000;279:L1159–L1171.
23. Cogo PE, Zimmermann LJ, Meneghini L, et al. Pulmonary surfactant disaturated-phosphatidylcholine (DSPC) turnover and pool size in newborn infants with congenital diaphragmatic hernia (CDH). *Pediatr Res*. 2003;54:653–658.
24. Merrell AJ, Ellis BJ, Fox ZD, Lawson JA, Weiss JA, Kardon G. Muscle connective tissue controls development of the diaphragm and is a source of congenital diaphragmatic hernias. *Nat Genet*. 2015;47:496–504.
25. Jesudason EC, Connell MG, Fernig DG, Lloyd DA, Losty PD. Early lung malformations in congenital diaphragmatic hernia. *J Pediatr Surg*. 2000;35:124–127. discussion 128.
26. Correia-Pinto J, Baptista MJ, Pedrosa C, Estevao-Costa J, Flake AW, Leite-Moreira AF. Fetal heart development in the nitrofen-induced CDH rat model: the role of mechanical and nonmechanical factors. *J Pediatr Surg*. 2003;38:1444–1451.
27. Ackerman KG, Herron BJ, Vargas SO, et al. Fog2 is required for normal diaphragm and lung development in mice and humans. *PLoS Genet*. 2005;1:58–65.
28. Danzer E, Davey MG, Kreiger PA, et al. Fetal tracheal occlusion for severe congenital diaphragmatic hernia in humans: a morphometric study of lung parenchyma and muscularization of pulmonary arterioles. *J Pediatr Surg*. 2008;43:1767–1775.
29. Takahashi T, Friedmacher F, Takahashi H, Hofmann AD, Puri P. Kif7 expression is decreased in the diaphragmatic and pulmonary mesenchyme of nitrofen-induced congenital diaphragmatic hernia. *J Pediatr Surg*. 2015;50:904–907.
30. van Loenhout RB, Tseu I, Fox EK, et al. The pulmonary mesenchymal tissue layer is defective in an in vitro recombinant model of nitrofen-induced lung hypoplasia. *Am J Pathol*. 2012;180:48–60.
31. Yamashita O, Yoshimura K, Nagasawa A, et al. Periostin links mechanical strain to inflammation in abdominal aortic aneurysm. *PLoS One*. 2013;8:e79753.
32. Rosselli-Murai LK, Almeida LO, Zagni C, et al. Periostin responds to mechanical stress and tension by activating the MTOR signaling pathway. *PLoS One*. 2013;8:e83580.
33. Ahlfeld SK, Gao Y, Wang J, et al. Periostin downregulation is an early marker of inhibited neonatal murine lung alveolar septation. *Birth Defects Res A Clin Mol Teratol*. 2013;97:373–385.
34. Bozyk PD, Bentley JK, Popova AP, et al. Neonatal periostin knockout mice are protected from hyperoxia-induced alveolar simplication. *PLoS One*. 2012;7:e31336.
35. Kuhn B, del Monte F, Hajjar RJ, et al. Periostin induces proliferation of differentiated cardiomyocytes and promotes cardiac repair. *Nat Med*. 2007;13:962–969.
36. Warburton D, Bellusci S, De Langhe S, et al. Molecular mechanisms of early lung specification and branching morphogenesis. *Pediatr Res*. 2005;57:26R–37R.
37. van Loenhout RB, Tibboel D, Post M, Keijzer R. Congenital diaphragmatic hernia: comparison of animal models and relevance to the human situation. *Neonatology*. 2009;96:137–149.
38. Beurskens N, Klaassens M, Rottier R, de Klein A, Tibboel D. Linking animal models to human congenital diaphragmatic hernia. *Birth Defects Res A Clin Mol Teratol*. 2007;79:565–572.
39. Kotecha S. Lung growth: implications for the newborn infant. *Arch Dis Child Fetal Neonatal Ed*. 2000;82:F69–F74.